Article

A human kinase yeast array for the identification of kinases modulating phosphorylation-dependent protein–protein interactions

Stefanie Jehle[1], Natalia Kunowska[2], Nouhad Benlasfer[1], Jonathan Woodsmith[1,2] (iD), Gert Weber[3,4] (iD), Markus C Wahl[3] (iD) & Ulrich Stelzl[1,2,5,*] (iD)

Abstract

Protein kinases play an important role in cellular signaling pathways and their dysregulation leads to multiple diseases, making kinases prime drug targets. While more than 500 human protein kinases are known to collectively mediate phosphorylation of over 290,000 S/T/Y sites, the activities have been characterized only for a minor, intensively studied subset. To systematically address this discrepancy, we developed a human kinase array in *Saccharomyces cerevisiae* as a simple readout tool to systematically assess kinase activities. For this array, we expressed 266 human kinases in four different *S. cerevisiae* strains and profiled ectopic growth as a proxy for kinase activity across 33 conditions. More than half of the kinases showed an activity-dependent phenotype across many conditions and in more than one strain. We then employed the kinase array to identify the kinase(s) that can modulate protein–protein interactions (PPIs). Two characterized, phosphorylation-dependent PPIs with unknown kinase–substrate relationships were analyzed in a phospho-yeast two-hybrid assay. CK2α1 and SGK2 kinases can abrogate the interaction between the spliceosomal proteins AAR2 and PRPF8, and NEK6 kinase was found to mediate the estrogen receptor (ERα) interaction with 14-3-3 proteins. The human kinase yeast array can thus be used for a variety of kinase activity-dependent readouts.

Introduction

Protein kinases represent one of the largest protein families in eukaryotes, with the 518 annotated human kinases comprising about 2% of the protein-coding genome (Manning *et al*, 2002; Ubersax & Ferrell, 2007). The kinase domain catalyzes the phosphorylation of mainly serine, threonine, and tyrosine residues. Already, over 290,000 phosphorylation sites in human proteins have been reported (phosphosite.org; 09/21). Phosphorylation of a protein can have a wide range of molecular effects, such as changes in activation status, conformation, localization, or interaction patterns. Phosphorylation underpins cellular signaling pathways and regulates diverse processes such as transcription, metabolism, the cell cycle, and proliferation. Consequently, dysregulated protein kinases often drive disease phenotypes, and elucidating kinase activity profiles (Ochoa *et al*, 2016), their substrate relationships (Tan *et al*, 2009a; Corwin *et al*, 2017; Needham *et al*, 2019) and their effects on cellular processes and phenotypes (Campbell *et al*, 2016) are imperative to better understand the mechanisms of disease progression. Multiple kinase inhibitors are used as first-line therapy in many cancers as well as in other diseases (Cohen *et al*, 2021). Despite the large number of human kinases with a pivotal role in cellular signaling, there is a well-documented research bias toward a small set of highly studied kinases such as p38a, SRC, EGFR, PKA, ERK1, KDR, ABL, CDK1, or KIT (Fedorov *et al*, 2010; Berginski *et al*, 2021). Studying kinase activity within cells is difficult, as kinases exhibit overlapping substrate specificity and differential expression, depending on the cell type, cell cycle phase, or subcellular localization, and have order(s) of magnitude differences in enzymatic activities. Furthermore, kinases form complex signaling networks that contain redundancy and feedback loops. Therefore, assaying kinase activity is typically done with purified kinase domains *in vitro* or with engineered biosensors (Shults *et al*, 2005; Zhang & Allen, 2007; Enzler *et al*, 2020; Schmitt *et al*, 2020). However, a versatile simple readout to analyze wild-type kinase activities in parallel at the

1 Otto-Warburg-Laboratory, Max-Planck-Institute for Molecular Genetics (MPIMG), Berlin, Germany
2 Institute of Pharmaceutical Sciences, University of Graz, Graz, Austria
3 Institut für Chemie und Biochemie, Freie Universität, Berlin, Germany
4 Helmholtz-Zentrum Berlin für Materialien und Energie, Macromolecular Crystallography, Berlin, Germany
5 Field of Excellence BioHealth, University of Graz and BioTechMed-Graz, Graz, Austria
*Corresponding author. Tel: +43 3163805397; E-mail: ulrich.stelzl@uni-graz.at

kinome scale would be a valuable complement to current approaches.

Human kinases have been shown to be active in yeast. For example, expression of human serine/threonine (S/T) cell cycle kinase CDK1 suppresses lethality of *cdc28* kinase mutant alleles in yeast (Elledge & Spottswood, 1991; Ninomiya-Tsuji *et al*, 1991). The yeast *kin28* deletion strain could be complemented by seven human paralog kinases (Yang *et al*, 2017). Also, active tyrosine (Y) kinases have been expressed in yeast to reveal kinase regulation mechanisms (Nada *et al*, 1991), identify protein–protein interactions (Grossmann *et al*, 2015), and study mechanism of kinase specificity (Corwin *et al*, 2017). Elevated expression of active human kinases quickly causes yeast growth defects. When expressing v-SRC, yeast growth was diminished (Brugge *et al*, 1987; Kornbluth *et al*, 1987; Cooper & MacAuley, 1988; Ahler *et al*, 2019) and later reports confirmed that human protein tyrosine kinase toxicity in yeast can be explained by aberrant phosphorylation of yeast proteins (Boschelli *et al*, 1993; Florio *et al*, 1994; Kritzer *et al*, 2018). Likewise, when human S/T kinase AKT1 is expressed in yeast it is phosphorylated on T308 and S473 and thus activated (Alessi *et al*, 1996). When AKT1 activity is increased either through oncogenic mutations or co-expression of the catalytic subunit of PI3 kinase, it causes increased growth inhibition of yeast cells (Rodríguez-Escudero *et al*, 2009). In order to set up a drug screening platform in yeast, Sekigawa *et al* utilized a human cDNA library which also contained human kinases for overexpression screening. About 23% of the tested kinases, including serine/threonine kinases, caused a visible growth defect of yeast under standard growth conditions (Sekigawa *et al*, 2010). Recently, screening of >500 human kinases revealed 28 kinases with strong overexpression-associated toxicity in yeast, which was further leveraged to screen for genetic suppressors of this growth defect (Kim *et al*, 2020).

Here, we aimed to systematically exploit the yeast growth phenotype caused by overexpression of active human kinases as an activity readout. While 15% of the 6100 *S. cerevisiae* genes are essential under standard growth conditions, approximately another 63% of the *S. cerevisiae* open reading frames (ORFs) were required for full growth when tested under more than 1000 different conditions (Hillenmeyer *et al*, 2008). In addition, essentiality of *S. cerevisiae* genes is strongly dependent on genetic interactions, which vary within different genotype of the strains (Dowell *et al*, 2010). This can be explained by the cellular protein interaction networks underlying the genotype to phenotype relationship, which are strongly modulated through genetic and environmental variation (Woodsmith & Stelzl, 2014; Filteau *et al*, 2016). Therefore, we hypothesized that the deleterious effects of aberrant phosphorylation of yeast proteins by human kinases may be further enhanced under nonstandard culture conditions and in different genomic backgrounds of different *S. cerevisiae* yeast strains.

We developed a human protein kinase yeast array that comprises more than 50% of the annotated human kinome and utilizes ectopic yeast growth as a simple readout for kinase activity in a living organism. Yeast growth is assayed with four strains with different genomic backgrounds and across a large variety of environmental conditions. Kinase activity is demonstrated growth assays in comparison with kinase-dead mutant versions and by assaying phosphorylation of yeast proteins directly with different phospho-substrate antibodies on whole yeast protein lysates. The yeast array is a versatile tool to broadly capture human kinase activity which can be coupled with any yeast assay available. Here, we demonstrate its utility by applying the array in identification of the kinases modulating known phosphorylation-dependent PPIs.

Results

An array of human protein kinases in budding yeast

To construct a large human kinase array in yeast and leverage yeast growth phenotypes as kinase activity readout under various conditions and different genetic backgrounds, we collected ORFs for 266 human protein kinases (Fig 1A). As a control group for the kinases, we employed 80 proteins, including 10 kinase-dead versions and 70 unrelated proteins without kinase domains. 92% of the proteins in the kinase set and control set were covered with two or more ORFs. We subcloned the ORFs into two yeast expression vectors, both under a weak Cu^{2+}-inducible yeast promoter, either with or without a nuclear localization sequence (Grossmann *et al*, 2015; Corwin *et al*, 2017), arriving at a total of 1017 different plasmids. The 266 protein kinases represented over a half of the known human kinome from all major groups and families of the Human Kinome Tree (Manning *et al*, 2002) (Fig 1B). The set also included five members of the atypical kinases that were shown to differ in some crucial sequence and structural features from the major group kinases (Kanev *et al*, 2019).

Figure 1. The human kinase yeast array.

A Schematic representation of the principle of the kinase yeast array and a flow diagram showing the construction of the human kinase array.

B The Human Kinome Tree representing 518 kinases in nine families (modified from (Manning *et al*, 2002) using CORAL at http://phanstiel-lab.med.unc.edu/CORAL/). Pie charts indicate the fraction of kinases contained in the human kinase yeast array. In total, 266 human protein kinases and 52% of the human kinome is represented in the array.

C Hierarchical clustering of the results of the yeast growth phenotype screen. In each strain, the 266 kinases were binned (0–4) according to the number of conditions in which the kinase caused a growth phenotype. Hierarchical clustering revealed sets of topmost (52), highly (98), and moderately active (116) kinases. Top 30 active kinases causing many growth phenotypes across all conditions-strain pairs are listed.

D Comparison of the fraction of kinases that result in a growth phenotype across all conditions-strain pairs. Kinases are grouped into 179 (67%) with a yeast ortholog and 87 (33%) human protein kinases without orthologous yeast kinases. The latter group includes 41 tyrosine kinases and 46 S/T kinases which were separated in the analysis. The former group contains both one-to-many and many-to-many orthologous kinases. Tyrosine kinases that strongly inhibited yeast growth and human kinases that are orthologous to yeast kinases were more likely to perturb yeast growth than human kinases without a yeast ortholog. Data are from a single large-scale growth measurement. The boxes extend from 1st to 3rd quartile with the central band representing the median. The whiskers extend to the furthest point up to 1.5 times the interquartile range away from the nearest quartile, with any further points marked as outliers. *P*-values are calculated using the Mann–Whitney test.
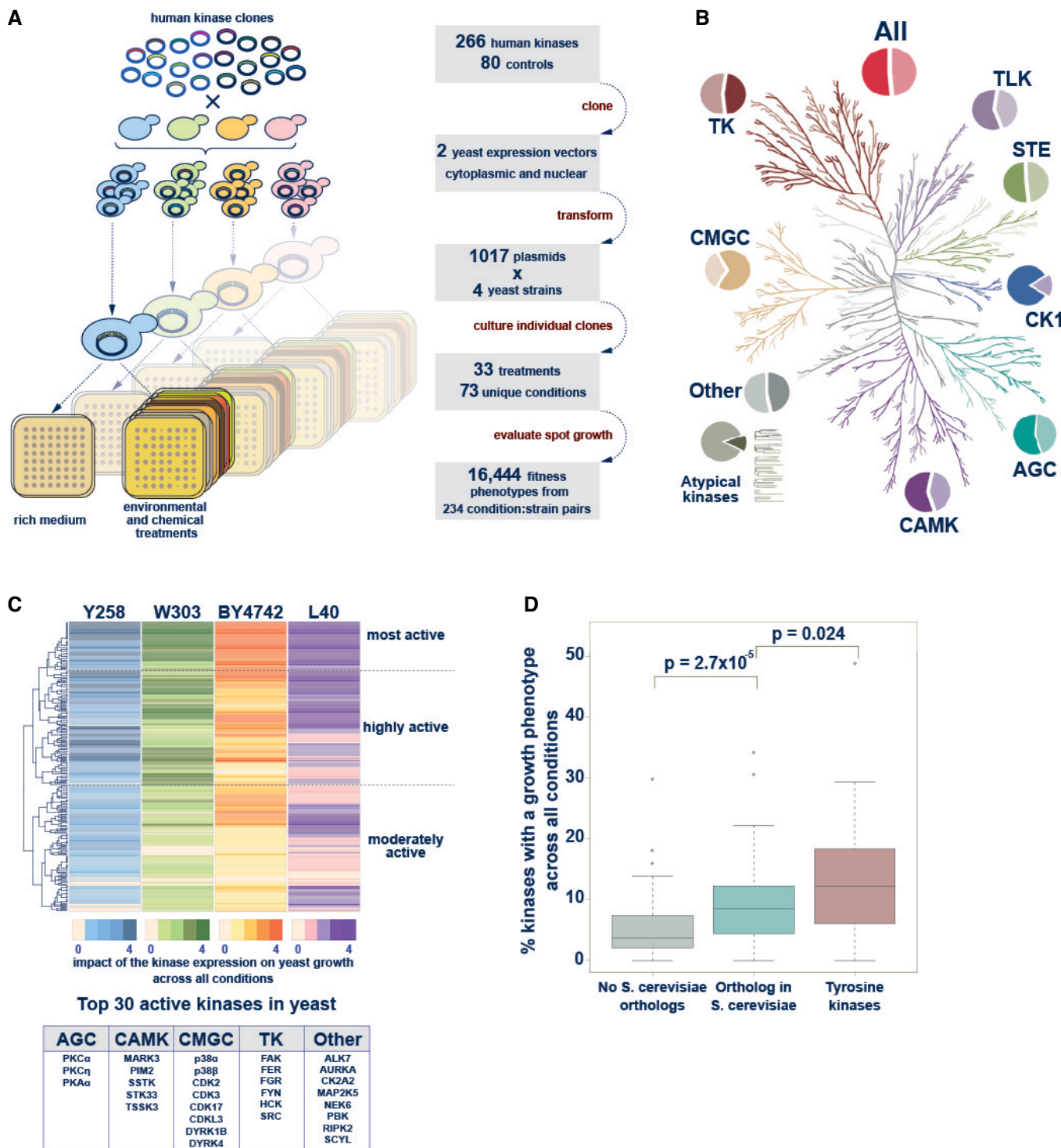
Figure 1.

The basic underlying principle of our kinase yeast array approach is that kinase activity will lead to aberrant phosphorylation of yeast proteins and thereby impair the yeast growth. In an initial test, the induction of kinase expression at 20 μM Cu^{2+} resulted in a yeast growth phenotype for 18% of the kinases. To be able to assay kinase activity using growth phenotypes as broadly as possible, we used four *S. cerevisiae* strains with different genomic backgrounds exhibiting different protein expression and growth phenotypes: the commonly used haploid laboratory strain BY4742 (MATα) (Winston *et al*, 1995; Brachmann *et al*, 1998), the haploid yeast two-hybrid (Y2H) strain L40c (MATa) (Worseck *et al*, 2012), the diploid strain W303 (MATa/MATα) (Ralser *et al*, 2012), and the haploid protein expression strain Y258 (MATa) (Newman *et al*, 2013). They were individually transformed with the two sets of

kinase plasmids. We then cultured these strains in parallel in a 384-array format on agar under various growth conditions (Fig 1A). The conditions included carbon sources other than glucose, the presence of detergents or denaturing agents, environmental triggers (pH, temperature), and addition of metal ions, osmotic stress agents, and other chemicals (such as $MnCl_2$, $K_3Fe(CN)_6$, or LiCl) to the growth media. Together, 33 unique treatments were assayed with additives in various concentrations adding up to a total of 73 different conditions in which at least one of the four strains were evaluated successfully (Dataset EV1). The evaluation of over 300,000 yeast spots for 266 kinases revealed that many kinases show growth reduction in at least one condition for one strain. Growth was evaluated on a 0–3 scale, reflecting none, weak, moderate, and severe growth reduction, respectively. When we plotted the number of kinases showing reduced growth per condition for each of the four strains, we observed bimodal distributions with very low counts between 150 and 200 kinases per condition, separating conditions with relative fewer, specific kinase signals from conditions that have a general diminishing effect on yeast growth. Therefore, conditions with reduced growth of more than 175 (17%) kinases were excluded from further analysis (Dataset EV2). A total of 243 condition-strain pairs were considered, with 41 conditions evaluated for all four strains and a total of 70, 62, 64, and 47 conditions for BY4742, L40c, W303, and for Y258, respectively (Dataset EV1). The use of different laboratory strains increased sensitivity as the majority of kinase-condition pairs with growth effect were detected in one strain only (Fig EV1). In total, 25, 36, 48, and 89 kinases with severe growth reduction were detected in, respectively, 4, 3, 2, and 1 yeast strain.

The 266 human protein kinases were then clustered based on their activity (Fig 1C). For that, the kinases were grouped in four bins, according to the number of conditions where they exhibit a growth phenotype and ranked separately for each strain (Dataset EV3). Hierarchical clustering revealed sets of kinases that were active in many conditions in one strain, and two or more strains, respectively. We grouped kinases according to their activity profiles across the four strains into three activity groups, from topmost active through highly to moderately active kinases (Fig 1C, Dataset EV4). In agreement with previous observations (Corwin et al, 2017), the topmost active kinases included cytoplasmic tyrosine kinases, which caused strong growth reduction when overexpressed in yeast. They also included two PKC family members (alpha and epsilon), two p38 MAP kinase family members (alpha and beta) as well as the cell cycle kinases CDK2, CDK3. Likewise, MARK3, RIPK2, NEK6, CDK17, CSNK2A2, AURKA, DYRK4, DYRK1B, and PKA were members of the high-activity group, with their expression frequently resulting in growth reduction (Fig 1C, box with the top 30).

Next, we compared the percentage of strong growth phenotypes caused by human kinases which have homologous kinase(s) in S. cerevisiae with human kinases that do not have homologs in yeast. Tyrosine kinases were treated as a separate group because tyrosine kinase signaling is a hallmark of multicellularity and did not evolve in yeast. Aberrant tyrosine phosphorylation can be toxic in yeast and it was suggested that organisms with evolved tyrosine signaling have a substantially reduced tyrosine content to prevent adverse tyrosine phosphorylation (Tan et al, 2009b). The results illustrate that the percentage of kinases causing a strong growth phenotype per condition is highest among the tyrosine kinases. The percentage of serine/threonine kinases causing a strong growth phenotype per

condition is higher for the human kinases with a homolog in yeast than for those without (Fig 1D). This on one hand confirms that high-level tyrosine phosphorylation in yeast is harmful, and on the other hand showed a significant trend suggesting that conserved S/T-kinases are more likely to interfere with essential yeast cellular process perturbing yeast growth than heterologous expression of nonconserved kinases.

Kinase activity is critical for yeast growth phenotypes

Evaluation of the yeast growth phenotype under a variety of growth conditions allowed monitoring the effects of the expression of individual human kinases through a simple readout such as colony size on agar. However, heterologous expression of any protein in yeast as such can affect yeast growth, independently of the activity of the expressed protein. Therefore, we asked whether kinase phosphorylation activity and not human protein overexpression per se drives our phenotypic readout.

We first compared the number of growth phenotypes caused by the human protein kinases with the number of growth phenotypes observed with the control set of proteins without kinase activity. The statistical comparison of the number of observed phenotypes for the two groups reveals that kinase expression resulted in growth defects much more often than the expression of unrelated proteins or phosphorylation-inactive kinase versions (Fig 2A).

To experimentally validate the impact of kinase activity on observed growth phenotypes in the yeast array, we monitored growth measuring the optical density of liquid cultures of wild-type kinase in parallel with kinase-dead mutant version over 24 h. The results for BUB1 and NEK6 illustrate that there is no difference in yeast growth under standard growth conditions in this assay. The addition of 3.2% DMSO to the media inhibited yeast growth, observable through a shallower growth curve and lower maximum cell density. In the presence of DMSO, the expression of the wild-type kinase of BUB1 or NEK6 diminishes yeast growth in comparison to the respective BUB1 (K821M) and NEK6 (K74M&K75M) kinase-dead mutants (Fig 2B). The comparison of yeast growth upon expressing either the activated form of PKCα (A25E) or the PKCα (K368R) kinase-dead mutant revealed pronounced differences under both standard and 3.2% DMSO growth conditions (Fig 2B). These results of this liquid growth assay were in good agreement with the results of the solid media screen, confirming that the kinase activity is required to inhibit yeast growth.

To directly show kinase activity in the yeast strains, we assayed kinases for their ability to phosphorylate endogenous yeast proteins using phospho-specific antibodies. To this end, whole-cell lysates from yeast expressing human kinases were subjected to SDS–PAGE and western blotting and probed with either a general phospho-tyrosine-recognizing antibody (4G10) or five different, commercially available phospho-substrate antibodies which recognize phosphorylated S/T sites with little amino acid sequence context specificity (Fig 2C). Equal amount of whole-cell lysate was probed comparing different kinases as well as kinases with the respective kinase-dead mutant variants. As illustrated for PKCα, p38α, AURKB, and FYN in Fig 2C, diverse patterns of immunoreactivity were obtained when probed with indicated antibodies. Most tyrosine kinases phosphorylated yeast proteins, albeit with different activity and specificity (Corwin et al, 2017). Endogenous serine and threonine
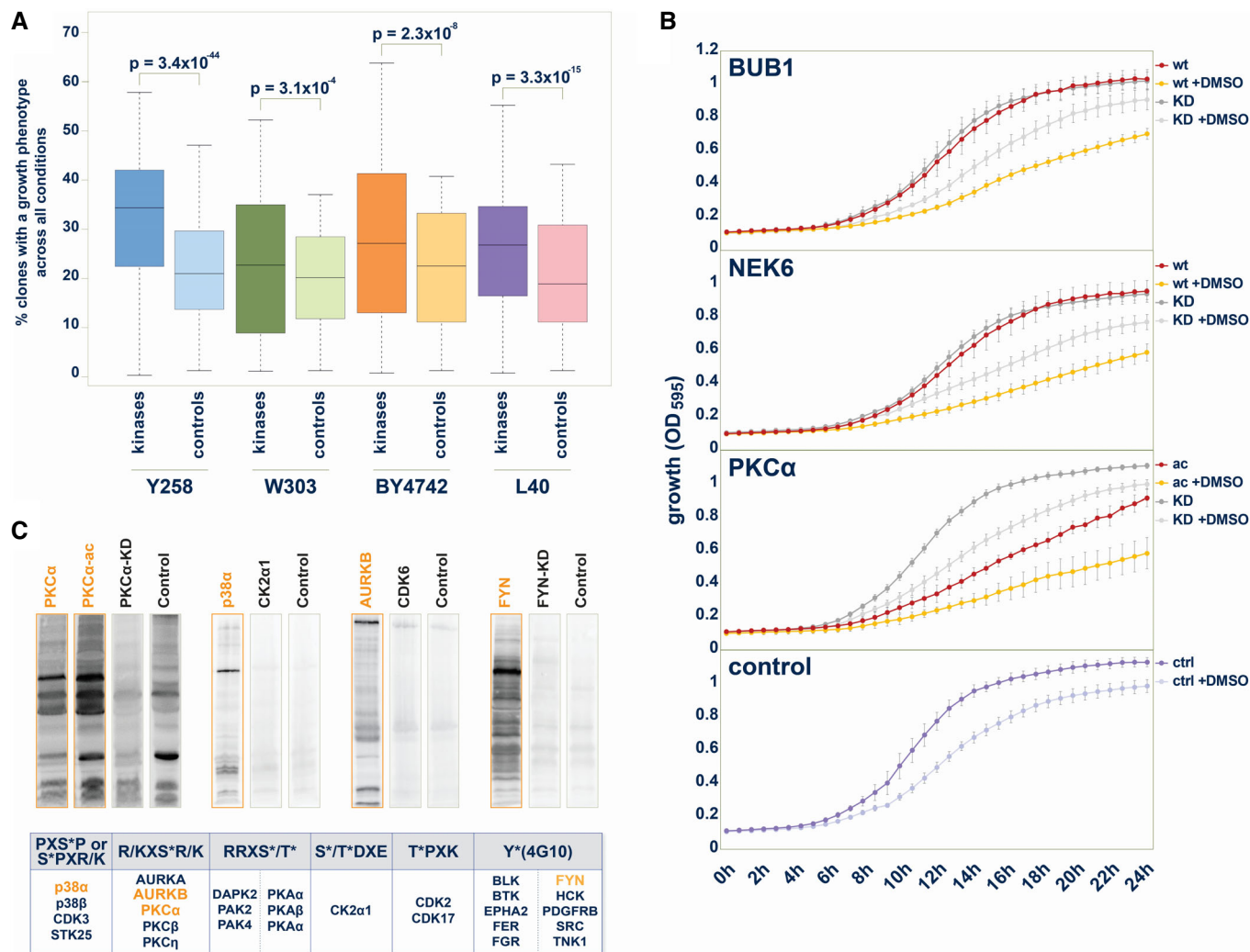
Figure 2. The yeast growth phenotype is a readout for the kinase phosphotransferase activity.

A   Statistical comparison of the number of yeast growth phenotypes between kinase group and control protein group. In each strain, across all conditions, the percentage of kinases that cause a phenotype upon exogenous expression is significantly higher than the percentage of control proteins, that cause a growth phenotype upon overexpression. Data are from a single large-scale growth measurement. The boxes extend from 1st to 3rd quartile with the central band representing the median. The whiskers extend to the furthest point up to 1.5 times the interquartile range away from the nearest quartile, with any further points marked as outliers. *P*-values are calculated using the Mann–Whitney test.

B   Growth comparisons of selected kinases with the kinase-dead mutant match. 24 h growth curves (OD$_{595}$) from liquid culture of yeast strains (W303) expressing human kinase in the presence or absence of 3.2% (v/v) DMSO. Upper panel: BUB1: BUB1 wild type, BUB1-KD: BUB1(K821M); upper middle panel: NEK6: NEK6 wild type, NEK6-KD: NEK6(K74M&K75M); lower middle panel: PKCα-ac: PKCα(A25E), PKCα-KD: PKCα(K368R); lower panel: Control with empty plasmid. Error bars represent SD from three biological replicates.

C   Human protein kinases phosphorylate large sets of yeast proteins. Upper panel: In total, 27 human protein kinases showed activity toward yeast proteins visible on western blots through enhanced reactivity with phospho-motif antibodies on yeast proteins in comparison to other human kinases, kinase-dead mutant versions, or vector control samples. Commercially available pS/T-antibodies with relatively low sequence specificities were chosen to enable detection of phosphorylation of the yeast proteome by human kinases. Lower panel: Examples of western blots with equal amount of whole yeast cell lysate from strains expressing human kinases loaded. When developed with the indicated phospho-motif-recognizing antibodies, immunoreactive bands indicated phosphorylation of yeast proteins.

phosphorylation in yeast is high. Therefore, phosphorylation patterns were distinguishable from background signals for only a subset of the tested kinases and antibodies. In total, 27 human protein kinases showed phosphorylation activity toward yeast proteins with one of the six available antibodies (Fig 2C). These experiments showed that human kinases are active in yeast and phosphorylate yeast proteins.

The kinase array is a versatile tool to study human kinase activities

Our array set up to study kinase activities revealed a set of 150 highly active kinases (most and highly active). This subset of the human kinome included representatives from all major kinase families (Fig 3A, Dataset EV4). Many well-characterized kinases are

known cancer drivers, and more than 340 human kinases are associated with at least one type of cancer (Piñero *et al*, 2021). Ninety-five of the highly active kinases overlap with this cancer kinase set (Fig 3B). One major strength of the yeast kinase array is that it also covers a large number of less well-studied or difficult-to-study kinases. One hundred and sixty-two kinases, nearly one third of the kinome, have been designated by the NIH as being poorly understood. As their role or biological function is largely unknown they are termed "dark kinases" (Berginski *et al*, 2021). Our array contained 72 dark kinases, 35 of which were in the group of highly active kinases (Fig 3C).

In general, studying kinases in their cellular environment is challenging, as kinase perturbation results in widespread pleiotropic cellular effects. In addition, many kinases are also highly tissue specific and/or low abundant, posing further challenges for the characterization of activities. We used protein abundance data from 31 tissues from the PAXdb (Protein Abundance Database), that provides normalized relative protein abundance data across many diverse mass spectrometry-based proteome studies (Wang *et al*, 2015). The kinome tree view shows that tissue-specific and low-abundance kinases are well covered in our array (Fig 3D, tissue expression, Fig 3E, average protein abundance). For example, two members each of the TSSK, MARK, or DRYK kinases, all highly active in yeast, belong to the dark, tissue-specific group of kinases with low expression. The activity of human kinases in the yeast array is largely independent of endogenous expression levels in human cells, thus enabling to study all candidate kinases equally well.
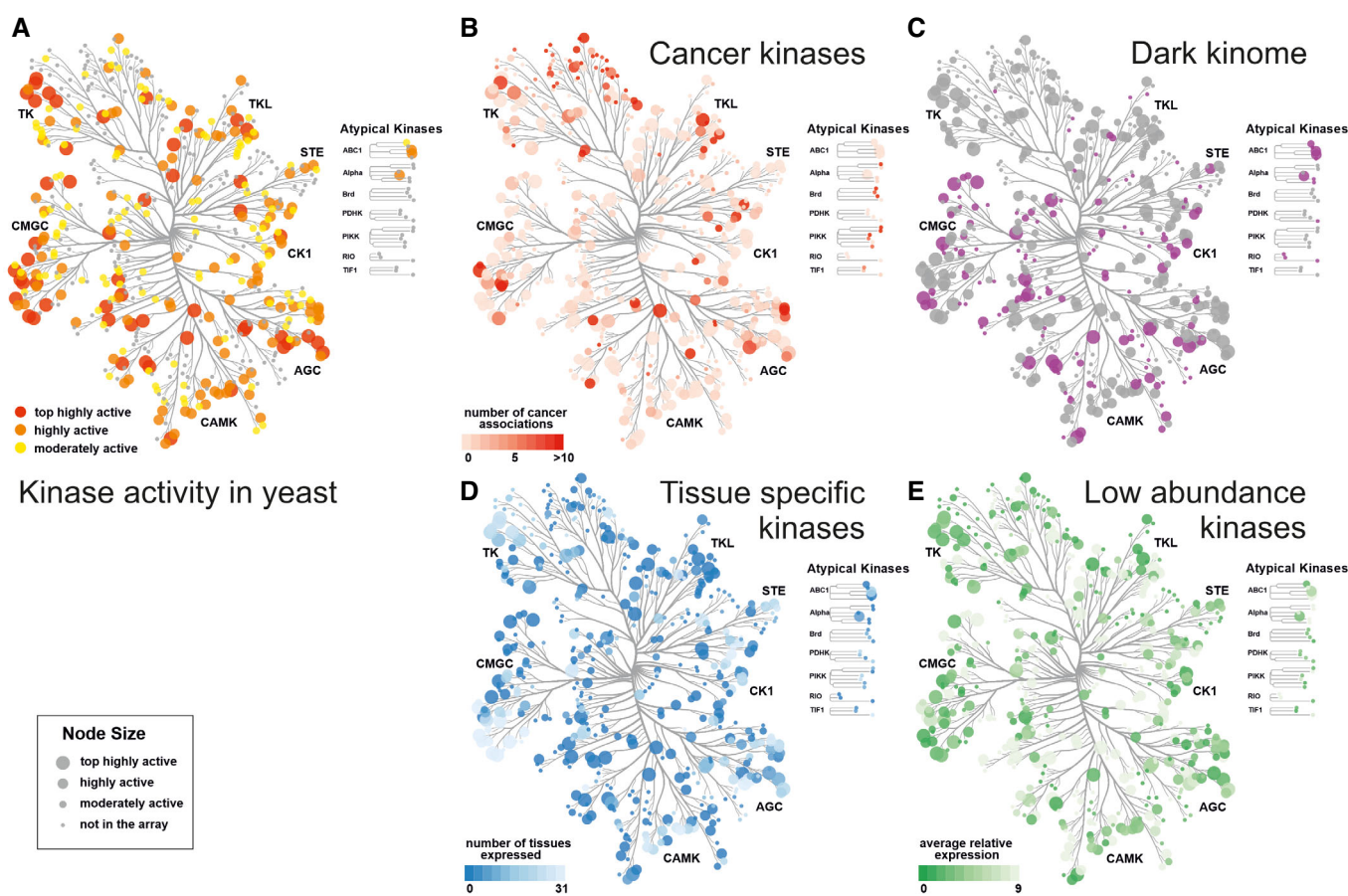

Figure 3. Representation of active human kinases in the yeast array.

A   Kinase activity in yeast. Kinase activity is played on the human kinome tree showing that all kinase families contain highly active kinases members.

B   Cancer kinases. The color-coded annotated cancer kinases overlap with highly active kinases (larger node size) in the array. 168 kinases in the array are linked to at least one cancer type (Piñero *et al*, 2021).

C   Dark kinases. Dark kinases (Berginski *et al*, 2021) in the kinome are color coded in purple, the tree shows the overlap of 35 highly active kinases (larger node size), and the total of 72 dark kinases represented in the array.

D   Tissue-specific kinases. Normalized proteomics data (Wang *et al*, 2015) from 31 tissues show that some kinases are only expressed in a few tissues. Many tissue-specific kinases (darker color) belong to the highly active kinases (larger node size) in the yeast array.

E   Low abundance kinases. Average relative expression levels over 31 tissues from PaxDB are color coded. Many kinases with low expression in mammalian cells (darker color) belong to the highly active kinases (larger node size) in the yeast array.

Data information: Panels A–E were prepared using CORAL at http://phanstiel-lab.med.unc.edu/CORAL/. Annotations are provided in Dataset EV4.

Phospho-yeast two-hybrid for identification kinases modulating PPIs

In our system, the activities of many human kinases can be monitored by growth reduction under varying conditions. However, low to moderate expression of human kinases under standard conditions does not impair yeast growth. Therefore, this kinase expression array opens avenues to alternative screening approaches, where the activity of a kinase can be assessed when coupled with any functional assay or readout in yeast. Cellular assays can involve drug inhibition/resistance selection, expression of a reporter such as luciferase, or expression of a fluorescent or epitope-tagged protein, or functional genomics readouts such as sequencing or mass spectrometry (Moesslacher *et al*, 2021). To explore the screening possibilities offered by the kinase array, we applied a phospho-yeast two-hybrid system (Grossmann *et al*, 2015) to identify kinases that modulate phosphorylation-dependent protein–protein interactions. The phosphorylation of one protein can either abolish its ability to interact with its partner, resulting in a loss of interaction, or it can enable the interaction with a second protein leading to a gain of interaction (Fig 4A). Both types of phosphorylation-dependent PPI switches require an active kinase facilitating the phosphorylation of one of the interaction partners. In the first setup where phosphorylation abolishes the Y2H interaction, active kinases are expressed from a third plasmid and phosphorylate either the bait or prey protein, resulting in reduced yeast growth on selective media. Conversely, the kinase activity can also promote yeast growth on selective media

when the kinase activity enables a protein complex formation (Fig 4A).

Modulation of protein interactions by phosphorylation has been widely described in the literature (Nishi *et al*, 2011), however, it often remains unclear which kinase(s) are responsible for interaction regulation. There are many "kinase-orphan" phosphorylation-dependent interactions described in the literature (Tudor *et al*, 2015) but no systematic approach tailored toward identifying kinases directly involved in phospho-mediated modulation of protein interactions has been reported. Our kinase array allows us to identify such kinases with a phospho-Y2H matrix approach (Fig 4B). A bait–prey pair of human proteins is co-expressed in one yeast strain (L40c **matα**) and mated with each of the L40c **mata** strains in the kinase array. The active kinases modulating the interaction of the two proteins of interest are then identified by altered yeast growth patterns (Fig 4A). To test the utility of this array in identifying biologically relevant kinase activities, we screened two well-characterized phosphorylation-dependent interactions, which represent the two cases and for which the responsible modulatory kinases are as yet unknown.

Kinase-dependent inhibition of the spliceosomal AAR2–PRPF8 interaction

PRP8 is a major constituent of the spliceosome, delivered as part of the U5 snRNP complex during the spliceosomal assembly cycle. AAR2 is a U5 snRNP and U4/U6-U5 tri-snRNP assembly factor. In
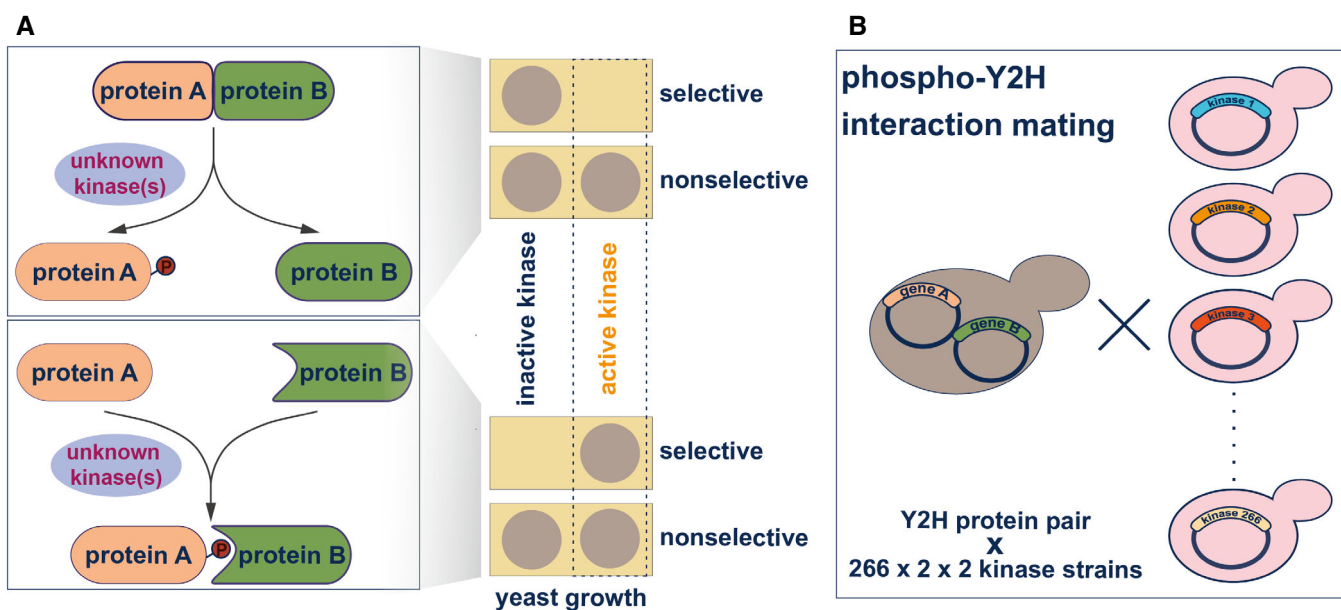

Figure 4. The human kinase yeast array as a tool to identify the kinase(s) modulating a phosphorylation-dependent PPI.

A   Two distinct cases of phosphorylation-dependent interaction modulation. Loss of interaction: the phosphorylation of one protein (A) by the active kinase results in the loss of interaction with the second protein (B) and, therefore, in no growth on selective media. Gain of interaction: Co-expression of an active kinase with a Y2H bait–prey protein pair can lead to phosphorylation of one protein partner (A) promoting the pS/T-dependent interaction with protein (B). In the phospho-Y2H approach, gain of interaction results in yeast growth on selective media.

B   Systematic phospho-Y2H interaction mating approach to identify the active kinase(s) modulating phosphorylation-dependent PPI. One yeast strain (L40matα) co-expressing the interacting bait and prey proteins and was mated against the 266 kinases in the array (L40mata) in a pairwise manner. The growth patterns of the diploid yeast strains that express bait, prey, and one kinase from a third plasmid, indicate phospho-modulation of protein interactions.

yeast, AAR2 is thought to dissociate from PRP8 at late assembly stages based on a phosphorylation trigger freeing PRP8 to allow for BRR2 binding (Fig 5A). While these events, including the crucial AAR2 phosphorylation site at serine 253, are well characterized in yeast (Weber *et al*, 2011, 2013; Galej *et al*, 2013), the kinase(s) responsible for the phosphorylation are unknown.

Here we investigate the phospho-dependent AAR2–PRPF8 interaction with the human proteins. The two proteins are conserved between yeast and human; however, it is not immediately evident from a standard sequence alignment whether the AAR2 phosphorylation sites including yeast serine 253 are conserved. The human AAR2–PRPF8 complex has been crystalized for high-resolution structure determination (Santos *et al*, 2015). We superimposed the two structures of the yeast and human Aar2/AAR2 protein and hypothesized that serine 284 in human may be functionally equivalent to serine 253 in yeast (Fig 5B). Notably, phosphorylation of the mammalian serine 284 is reported in PhosphoSitePlus (Hornbeck *et al*, 2012). Next, we recapitulated the interaction-disrupting effect of S253 phosphorylation observed in *S. cerevisiae* with the human orthologs using a Y2H approach (Fig 5C). Human PRPF8 bait (aa1755-2335) interacts with full-length human AAR2 prey using our standard Y2H system (Hegele *et al*, 2012; Worseck *et al*, 2012). While the S284A AAR2 mutant version has no effect, the S284E phospho-mimetic mutant in AAR2 abolished the Y2H growth read-out (Fig 5C). In a control experiment, we assayed a second candidate phospho-site, T356A and T356E AAR2 mutant versions (Weber *et al*, 2011), also in combination with S284E, which confirmed that the S284 phospho-mimetic version of AAR2 was sufficient to abolish binding of PRPF8 in the human system (Fig 5C). When immunoprecipitating the human PRPF8 RNase H-like domain fragment from transfected HEK293 cells, both the wild-type AAR2 and the nonphosphorylatable S284A mutant versions showed comparable binding, while the S284E phospho-mimetic mutant completely abolished the interaction (Fig 5D).

In order to identify candidate human kinases that can mediate this phosphorylation-dependent PPI switch, we screened each of the 266 kinases for loss of the Y2H signal (Fig 5E). We transformed L40c **matα** with the PRPF8-AAR2 bait and prey plasmids and mated this strain against the validated L40c **mata** kinase array. Each diploid strain expressed the two interacting proteins as well as one human kinase. After transfer on selective media, we identified two candidate kinases SGK2 and CK2α1 (CSNK2A1), that reproducibly had a negative effect on Y2H reporter-dependent yeast growth (Fig 5E). Because Y2H utilizes a transcriptional reporter system, which has high sensitivity also to transient and less stable interactions (Vinayagam *et al*, 2010), we do not expect that this setup will lead to complete loss of the signal. Rather, reduced, substoichiometric phosphorylation of AAR2 may well account for the observed decrease in yeast growth of the SGK2 and CK2α1 strains.

To validate the kinase array phospho-Y2H results, AAR2 and PRPF8 were tested in a co-expression and immunoprecipitation assay in HEK293 cells. Co-expression of either SGK2 or CK2α1 reduced the amount of wild-type AAR2 co-immunoprecipitated with PRPF8 in comparison to the nonphosphorylatable mutant S284A (Fig 5F). Together, these experiments in mammalian cells support the results obtained with the kinase array when coupled with the phospho-Y2H assay. Active SGK2 and CK2α1 kinases substantially reduced the spliceosomal assembly complex interaction of AAR2 and PRPF8, and may thus be involved in triggering the interaction switch of PRPF8 from AAR2 to BRR2 in mammalian cells.

Kinase-dependent interaction of ERα and 14-3-3 proteins

We next sought to test the utility of the kinase array in identification of kinases that promote protein–protein interactions. Estrogen receptor alpha (ERα), the hormone (β-estradiol)-sensing nuclear receptor frequently overexpressed in breast cancer, is heavily posttranslationally modified, including 26 phosphorylated residues (Hornbeck *et al*, 2012). Interestingly, De Vries-van Leeuwen *et al* reported that ERα dimerization is inhibited through a phosphorylation-dependent interaction of the ERα monomer with 14-3-3 proteins. Mediated by the ERα C-terminal phospho-threonine 594, the interaction prevents the activation of ERα-dependent transcription (Fig 6A), yet kinases which direct this inhibitory action remain elusive (Vries-van Leeuwen *et al*, 2013).

Figure 5. Identification of human S/T kinases modulating the AAR2–PRP8 protein interaction.

A   Schematic of phospho-dependent interaction of the spliceosomal AAR2 and PRP8. AAR2, a spliceosomal assembly protein, and PRP8 from a stable complex, which dissociates upon phosphorylation of AAR2. PPR8 is then free to bind the spliceosomal interaction partner protein BRR2 (Galej *et al*, 2013; Weber *et al*, 2013). This regulatory interaction switch is thought to be conserved between yeast and human. A protein kinase that can modulate the dissociation of AAR2 from PRP8 is unknown.

B   Superposition of the yeast Aar2 (orange, PDB entry 3SBT; (Weber *et al*, 2011)) 3D structure and a homology model of human AAR2 derived from HHpred (marine), based on the yeast Aar2p structure (Santos *et al*, 2015). The inset on the right shows a close-up view of the C-terminal domain, where serines 253 (yeast) and 284 (human) are displayed as sticks. Residues 154–170 and 318–356 of yeast Aar2 as well as residues 1–18, 170–201, and 359–384 of human AAR2 are not shown for clarity.

C   Y2H interaction experiment with human AAR2 (FL) as bait and PRP8 (aa1755-2335) as prey. Growth on selective media is abolished when AAR2 carries a S284E phospho-mimicry amino acid substitution. Mutation of second candidate phospho-site, AAR2(T356), does not influence the AAR2–PRP8 protein interaction.

D   Interaction of AAR2 and PRP8 in human cells. HA-tagged PRP8 (aa1755-2335) was co-expressed in HEK293 cells with either wild-type AAR2, AAR2(S284A) or AAR2 (S284E) mutant versions. Immunoprecipitation of PRP8 led to a coprecipitation of wild-type AAR2 and phospho-null AAR2(S284A). In contrast, the phospho-mimicry AAR2(S284E) version did not bind PRP8.

E   Results of the phospho-Y2H screen to identify kinases modulating the interaction of AAR2 and PRP8. Growth on selective media (SD5), of strains carrying AAR2 bait and PRP8 prey plasmids is reduced through co-expression of either SGK2 or CK2α1(CSNK2A1). Growth reduction is visible in a 1:10 dilution series on selective agar (SD5) in comparison to the control media (SD3). Ctrl: nonrelated kinases.

F   Interaction of AAR2 and PRP8 in human cells in the presence of SGK and CK2α1 kinases. Experiment as in (D). Co-expression of wild-type SGK2 and CK2α1 reduces the amount of AAR2 co-immunoprecipitated with RPR8.
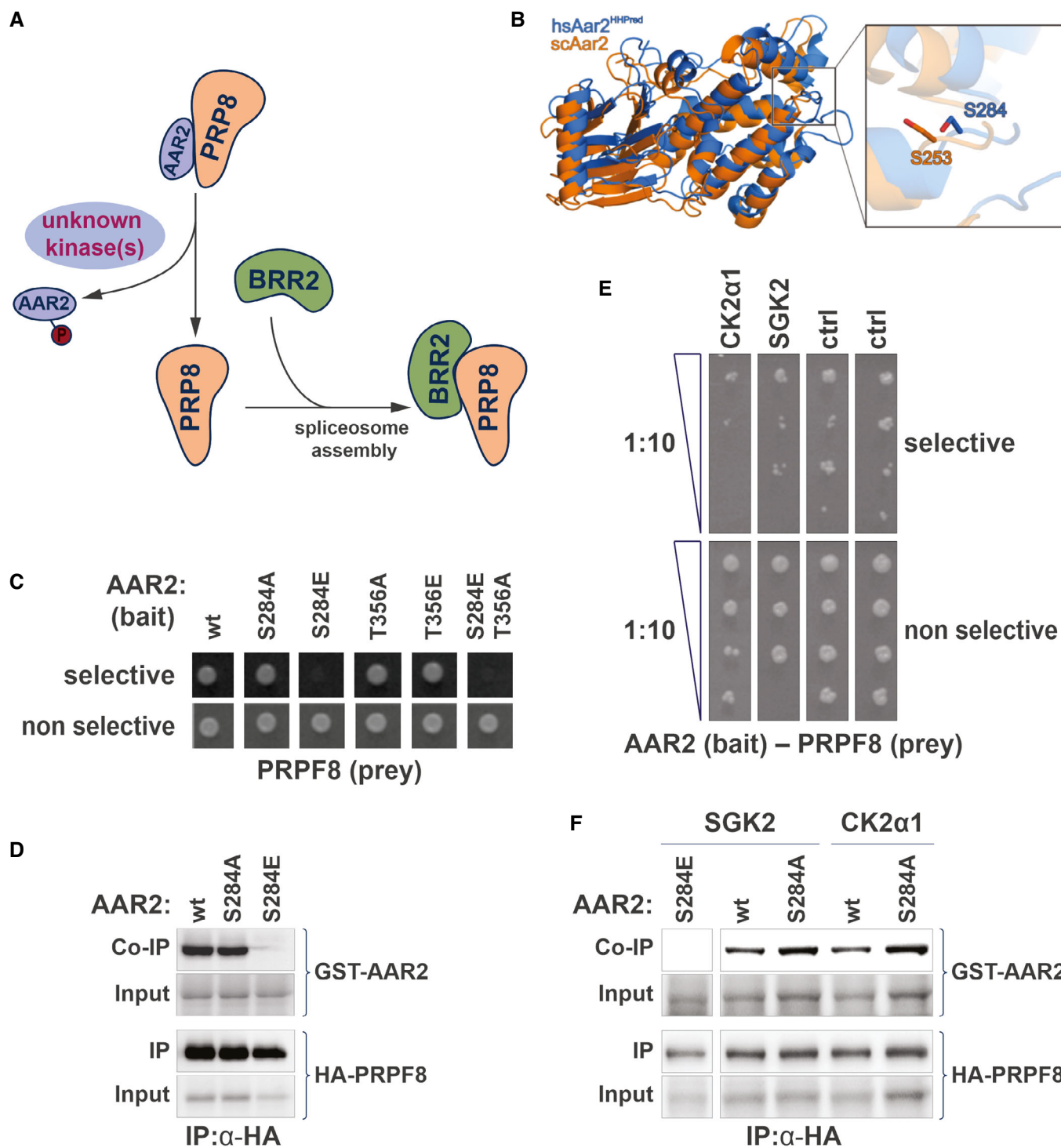
Figure 5.

For phospho-Y2H analysis, we cotransformed L40c **matα** with ERα bait and 14-3-3 prey constructs for interaction mating with the human kinase yeast array. While ERα did not show interaction with 14-3-3β across multiple replicas in a classical Y2H experiment in the absence of a kinase (Fig 6B, Ctrl), the kinases BUB1, NEK6, CDK17, and PAK5 were able to reproducibly promote the interaction as indicated by the

yeast growth on selective agar (Fig 6B). Parallel screening of NEK6 (K74M&K75M), PAK5(K478M), BUB1(K821M), and CDK17(K221M) kinase-dead mutants suggested that phosphotransferase activity is required to promote the ERα–14-3-3β interaction for the kinases NEK6 and BUB1. In contrast, kinase-dead mutants of PAK5 and CDK17 still promoted growth on Y2H selective medium (Fig 6B).
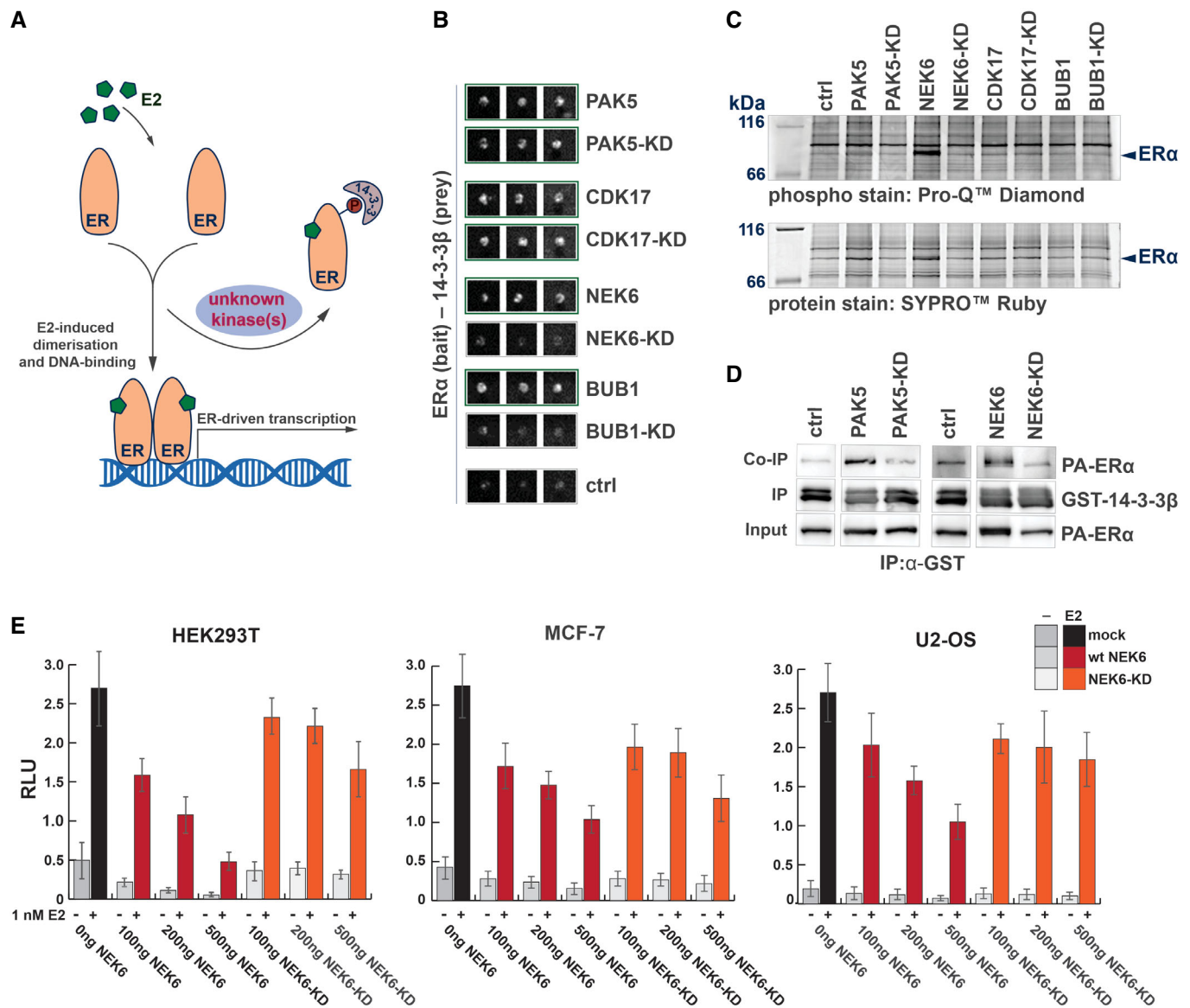
Figure 6.   Identification of human S/T kinases modulating the ERα-14-3-3 phosphorylation-dependent interaction.

A   Schematic of phospho-dependent interaction of the estrogen receptor ERα with 14-3-3β. Phosphorylation of ERα promotes its interaction with 14-3-3 proteins. This interaction removes ERα from the E2-stimulated ERα dimerization and consequently inhibits Erα–DNA interactions and gene expression. A protein kinase that can modulate the binding of ERα to 14-3-3 proteins is unknown.

B   Results of the phospho-Y2H screen to identify kinases modulating the interaction of the ERα with 14-3-3β. The interaction of ERα (prey) with 14-3-3β (bait) is promoted by the co-expression of wild-type kinases of PAK5, CDK17, BUB1, and NEK6, visible by the yeast growth on selective media in comparison to the control (three biological replicas are shown). The co-expression of the kinase-dead mutants of PAK5 and CDK17 also promoted the interaction of ERα and 14-3-3β. In contrast the kinase-dead mutant versions of BUB1(K821M) and NEK6(K74M&K75M) did not promote the Y2H interaction.

C   Phosphorylation of ERα in mammalian cells. ERα was co-expressed with the indicated wild-type kinases or kinase-dead versions in HEK293 cells and immunoprecipitated. Phosphorylation status of ERα was analyzed with an in-gel phosphostain (Pro-Q® Diamond phosphoprotein gel stain, Invitrogen), relative to the whole-protein stain (SYPRO®Ruby protein gel stain, Invitrogen).

D   Interaction of ERα and 14-3-3β in a GST pull-down assay. GST-tagged 14-3-3β was expressed in E. coli and immobilized on beads. PA-tagged ERα was co-expressed with either wild-type PAK5 or NEK6, the kinase-dead (KD) version or without a kinase in HEK293 cells. Immobilized 14-3-3β was used to pull PA-tagged ERα from the HEK lysates. Coprecipitation of ERα was successful in the presence of wild kinases, but not in their absence or with kinase-dead mutant versions.

E   Effect of NEK6 co-expression on ERα gene activation. Relative luciferase activity of ERα in the presence and absence of 1 nM E2 (17β-estradiol) was measured. A dose-dependent reduction (ng plasmid transfected) in E2-Erα-dependent luciferase expression was observed in HEK293T, MCF-7, and US-OS cancer cell lines. This effect was not observed with the NEK6(K74M&K75M) kinase-dead version. Graphs represent ≥ 5 biological replicates, each derived from averaging six technical replicates. Error bars indicate SD across the biological replicates.

Up to 40% of the human kinome was predicted to bind to 14-3-3 proteins (including CDK17), and about 30 human protein kinases, including PAK5, have been shown to directly bind 14-3-3 proteins (Tinti *et al*, 2014). As PAK5 and CDK17 can potentially bind both ERα and 14-3-3, they may form a relatively stable ternary complex and, therefore, drive the positive Y2H signal in a phosphorylation-independent manner. To test this hypothesis, we performed a co-immunoprecipitation assay with a luciferase-based readout with 14-3-3β and wild-type as well as kinase-dead mutants of BUB1, NEK6, PAK5, and CDK17. The results indicated that the kinases PAK5 and CDK17 were able to bind to 14-3-3β while there no was binding detected for the wild-type or kinase-dead mutants of BUB1 or NEK6 (Fig EV2). Together with the phospho-Y2H results using kinase-dead mutants, these results are consistent with a model whereby PAK5 and CDK17 drive the Y2H interaction through formation of more stable ternary complexes with ERα and 14-3-3, while BUB1 and NEK6 promote Erα–14-3-3 interaction mainly through phosphorylation.

To analyze whether the co-expression of the kinases BUB1, NEK6, PAK5, and CDK17 in HEK293 cells results in an increased phosphorylation of ERα, the phosphorylation status of ERα was determined with an in-gel phospho-stain. While no kinase activity of CDK17 and BUB1 could be detected on ERα after immunoprecipitation, the kinases NEK6 and PAK5 promoted the phosphorylation of ERα, in comparison to the corresponding kinase-dead mutants or the control sample without kinase overexpression (Fig 6C). A pulldown assay with bacterial-expressed GST-tagged 14-3-3β resulted in ERα binding if co-expressed with the wild-type kinases NEK6 or PAK5 in HEK293 cells when compared to the kinase-dead mutant co-expression or negative control experiments (Fig 6D). This result is consistent with the observed ERα-phosphorylation activity of NEK6 and PAK5 in HEK293 cells.

To summarize, NEK6 and BUB1 promote the association of 14-3-3β and ERα in Y2H in a kinase activity-dependent manner, and do not directly interact with 14-3-3β themselves. When co-expressed in mammalian cells, active forms of NEK6 and PAK5 increase the phosphorylation of ERα and its direct binding to 14-3-3β in GST pulldown assays. Together, these protein interaction data point to NEK6 as a prime candidate to regulate the association of ERα with 14-3-3β and thereby its transcriptional activity *in vivo*. To test this hypothesis, we transfected HEK293T cells with ERα and ERα-dependent luciferase reporter harboring three copies of Estrogen Response Element in front of a minimal promoter and a luciferase gene (3xERE-LUC, (Hall & McDonnell, 1999)), in the presence of increasing amounts of wild-type or kinase-dead NEK6. The cotransfection of active NEK6 kinase inhibited estrogen-driven activation of the luciferase reporter in a dose-dependent manner (Fig 6E). The observed effect was dependent on the kinase activity of NEK6, as the attenuation of ERα transcriptional activity was negligible with the kinase-dead NEK6-KD version. Expression of NEK6 did not affect the cell cycle (Fig EV3). The inhibition was reproduced in MCF7 cells, a breast cancer cell line, and a standard model to study ERα transcriptional activity. Finally, also in U2-OS cells, the osteosarcoma cell line originally used by De Vries-van Leeuwen *et al* to demonstrate the effects of 14-3-3 binding, active NEK6 kinase also reduced the ERα-dependent reporter gene transcription (Fig 6E). These results, obtained in three relevant mammalian cell lines, functionally support the results of our human kinase array screening approach, suggesting that NEK6 is a prime candidate kinase that can promote phosphorylation of ERα and its interaction with 14-3-3 proteins.

Discussion

Kinase activity drives signaling processes and, when deregulated, human diseases. Kinases are the third largest group of human protein drug targets, and kinase inhibitors represent the largest fraction of drugs with poly-pharmacological effects, that is, they act through multiple targets (Cohen *et al*, 2021). However, beyond their primary sequence and domain architecture, a large fraction of human kinases are hardly characterized (Fedorov *et al*, 2010; Berginski *et al*, 2021). Systematic assaying multiple kinases activities in parallel is, therefore, fundamental to improve our understanding of cellular signaling, disease processes and drug action (Fedorov *et al*, 2010; Elkins *et al*, 2016).

Experimental methods for assaying kinase activities include *in vitro* assays with recombinant proteins (Anastassiadis *et al*, 2011; Elkins *et al*, 2016) or the application of kinase-specific biosensors that work in cells (Shults *et al*, 2005; Enzler *et al*, 2020; Schmitt *et al*, 2020). For example, an enzyme assay panel employing more than 200 recombinant kinases was used with microfluidics capillary electrophoresis technology to screen for small-molecule inhibitors (Elkins *et al*, 2016). Because results using recombinant kinases *in vitro* do not always recapitulate *in vivo* conditions, other approaches prove valuable to assay kinase activities. Taipale *et al* (2013) used the interaction of HSP90 / CDC37 chaperones with kinases as thermodynamic sensors of kinase activity or inhibitor binding in a cell culture co-IP approach. Also, fluorescent biosensors examining conformational changes in kinase allow to temporally and spatially resolve kinase activities toward engineered targets in cells, tissues, and, to some extent, in whole organism (Zhang & Allen, 2007; Enzler *et al*, 2020; Schmitt *et al*, 2020). Clearly, accessible tools to study active kinases under cellular conditions are a useful addition to current approaches.

This study presents information about the activity of 266 human protein kinases obtained from a yeast array, using growth as a readout (Moesslacher *et al*, 2021). While most kinases when expressed at low levels in yeast do not bestow a growth phenotype, we have increased sensitivity of the growth readout by employing a variation of growth conditions and by using four distinct yeast strains. Comparison to a set of nonactive kinases and unrelated proteins indicated that although some phenotypes might be related to protein overexpression, this effect was not dominant. Moreover, some kinases may not be active in yeast because of the lack of regulatory proteins, or conversely, we may miss the activity of a set of kinases, where phosphorylation of yeast proteins simply is not detrimental to growth. For example, even though SGK2 and PAK5 were both grouped with the moderately active kinases, they could be identified from the array as candidates for modulating pS/T-PPIs because of the use of an alternative phospho-Y2H readout.

Examination of the yeast array yielded 150 highly active kinases. Our active kinase set is representative of the kinase families (Fig 3) and covers 35 members of the dark kinome (Berginski *et al*, 2021), including CDK17, NEK6, and MARK3. The human kinase array can be leveraged for a variety of assays, provided the activity of a kinase

can be coupled with a growth selection or other readouts. As proof of principle, we used the array to identify kinases that can modulate known pS/T-dependent protein interactions in a phospho-Y2H screen. While approaches exist to define phospho-mediated PPIs (Grossmann et al, 2015), the kinases that modulate the PPI often remain elusive and so far, no systematic approach to identify them is available. Our phospho-Y2H approach is highly scalable (Weimann et al, 2013; Woodsmith et al, 2017), however, it requires prior knowledge on phospho-modulated protein interactions, which is dispersed in the literature.

Here, we first addressed the interaction of the spliceosomal protein PRPF8 and the snRNP assembly factor AAR2. We showed that phosphorylation of S284 of human AAR2 disrupts the interaction with PRPF8 (Fig 5), which in analogy to yeast is thought to constitute an important step in U5 snRNP and U4/U6-U5 tri-snRNP biogenesis (Weber et al, 2011, 2013). The spliceosome is the large macromolecular protein-RNA complex that catalyzes pre-mRNA splicing. It assembles and disassembles on each pre-mRNA in a highly coordinated, stepwise manner governed by multiprotein–RNA interactions (Wahl et al, 2009; Hegele et al, 2012). In yeast, cytoplasmic assembly of the U5 snRNP includes the assembly factor Arr2 in place of the spliceosomal helicase Brr2, which requires tight regulation (Absmeier et al, 2015). There, the binding of Arr2 to Prp8 blocks the Prp8-binding site of Brr2. As the Brr2–Prp8 interaction is blocked, Brr2 helicase activity may be shut off during this phase of U5 snRNP assembly. Nuclear phosphorylation of Aar2 disrupts its interaction with Prp8 and allows incorporation of Brr2 into U5 snRNP, and subsequently the U4/U6-U5 tri-snRNP through which Brr2's helicase function is eventually delivered to the spliceosomal precatalytic B complex (Galej et al, 2013; Weber et al, 2013). Subject to further scrutiny, a similar phosphorylation-dependent regulation of the AAR2-PRPF8 interaction is also thought to play a role in U5 snRNP or U4/U6-U5 tri-snRNP assembly in human. The kinase that could contribute to this regulation is presently unknown.

Screening the L40c yeast kinase array for a loss of the Y2H AAR2-PRPF8 bait–prey interaction revealed that the kinases SGK2 and CK2α1 are able to reduce the interaction (Fig 5). This result was confirmed by co-immunoprecipitation assays in HEK293 cells, where co-expression of wild-type SGK2 or CK2α1 reduced the amount of AAR2 coprecipitated with PRP8. The AGC kinase group member SGK2 is not characterized very well. SGK kinases, just like AKT/PKB kinases are activated by PDK1 through phosphorylation of conserved residues (Kobayashi & Cohen, 1999). SGK2 is known to be involved in the phosphorylation of diverse set of cellular channels and receptors (Pao, 2012) including V-ATPase proton pump (Ranzuglia et al, 2020). The other candidate CK2α1, however, is a constitutively active kinase primarily located in the nucleus and thus could support disruption of the AAR2–PRPF8 interaction in the nucleus during late stages of U5 or U4/U6-U5 assembly. CK2α1 has been reported to phosphorylate a vast number of substrates and to regulate numerous cellular processes (Meggio & Pinna, 2003; Filhol & Cochet, 2009; Nuñez de Villavicencio-Diaz et al, 2017), including cell cycle progression, apoptosis, and transcription, as well as a viral infection. It is involved in other spliceosomal processes such as the phosphorylation of Prp3 (Dörr et al, 2008; Lehnert et al, 2008), the exon junction complex member / splicing activator RNPS1 (Trembley et al, 2005), and is associated with the U4/U6/U5 tri-snRNP complex (Meggio & Pinna, 2003).

Estrogen receptor alpha (ERα / ERS1) is one of the most highly studied hormone-sensing nuclear receptors. Its dimerization is essential for its ligand-dependent transcriptional activity. Blocking ERα function is the major route to treat luminal (ER$^+$) breast cancer. ERα is phosphorylated at various sites, and potential functions and protein kinases for some phosphorylation sites have been characterized (Anbalagan & Rowan, 2015). A phosphorylation-dependent interaction between ERα and the phospho-binding adaptors 14-3-3, which reduces the transcriptional activity and the proliferative effect of ERα in cells has been reported. The authors specifically demonstrated that phosphorylation of ERα is required for the binding of 14-3-3 protein and proposed that stabilization of this interaction with its effect on ERα transcriptional activity may be of therapeutic value (Vries-van Leeuwen et al, 2013).

We identified four candidate kinases, BUB1, NEK6, PAK5, and CDK17, with the ability to promote the interaction of ERα with 14-3-3β in a phospho-Y2H matrix approach from screening the kinase L40c array (Fig 6). In this assay, kinase activity of BUB1 and NEK6 was required to promote the interaction, whereas kinase-inactive versions of PAK5 and CDK17 were also sufficient for a positive Y2H growth readout. The latter results are explained by the ability of the two kinases to stably bind to 14-3-3 proteins. This binding is reported in the literature (Tinti et al, 2014) and was confirmed in luciferase-based co-immunoprecipitation experiments. However, we detected increased phosphorylation of ERα phosphorylation in HEK293 cells upon co-expression of wild-type NEK6 and PAK5 kinase. Expression of these two kinases also led to successful co-immunoprecipitation of ERα with 14-3-3β. In order to demonstrate that NEK6 phosphorylation-dependent increase of ERα–14-3-3 interaction can have functional consequences in cells, we performed ERα-dependent transcription activation assays. In all three cell lines tested, HEK293, the breast cancer cell line model MCF-7, and U2-OS cells, overexpression of the active NEK6 kinase reduced transcriptional activity in a dose-dependent manner, an effect not observed with the kinase-inactive NEK6 variant.

Among the four candidate kinases with the potential to modulate ERα activity via a phosphorylation-dependent interaction with 14-3-3 proteins we have identified, BUB1 is a fairly well-characterized kinase involved in spindle checkpoint control (Kang et al, 2008). In contrast, PAK5, CDK17, and NEK6 belong to the group of understudied, less well-characterized kinases. PAK5 (formerly PAK7) is an actin- and microtubule-associated, p21$^{cdc42/rac1}$ -activated kinase family member (Cau et al, 2001), which has been shown to promote proliferation, invasion, and migration of various cancer cell models (Huang et al, 2020). CDK17 (also PCTAIRE2) is an uncharacterized member of the cyclin-dependent kinase family (Malumbres et al, 2009). Taken together, our data point to NEK6, a cell cycle kinase involved in progression through mitosis (Yin et al, 2003; O'Regan & Fry, 2009), with only few substrates known so far (van de Kooij et al, 2019), as the strongest candidate as ERα effector.

Conclusion

Here, we built on the observation that heterologous expression of human kinases in yeast can cause a growth defect attributed to the

enzymatic phosphotransferase activity of these proteins (Sekigawa *et al*, 2010; Kim *et al*, 2020; Moesslacher *et al*, 2021). We have demonstrated that a large fraction of human kinases (56%) is active in our yeast array. For a subset of kinases, we have also demonstrated the kinase activity directly using kinase-dead mutant version as comparisons, or through monitoring the extent of yeast protein phosphorylation with phospho-specific antibodies. Mechanisms that explain why aberrant phosphorylation of yeast proteins impar yeast growth are largely elusive and may be different from kinase to kinase. Whether or not kinase activity can be reported using the yeast array depends on growth conditions, the yeast strain and the readout used. Readouts where kinase activity is coupled with growth inhibitory effects, either directly or via a reporter system, can be used to study kinase perturbation (Ahler *et al*, 2019) and inhibition (Nada *et al*, 1991; Koyama *et al*, 2006; Harris *et al*, 2013; Kim *et al*, 2020). Under conditions of low kinase expression levels that do not impair growth, different setups can be utilized to pick up kinase activities, for example, mass spectrometry-based substrate identification (Corwin *et al*, 2017) or screens for pY-dependent protein interactions (Grossmann *et al*, 2015). Here, we extended the phospho-Y2H approach to S/T kinases for the first time, utilizing the array to identify kinases that can modulate known pS/T-dependent protein interactions. Knowledge of potential kinases that regulate phospho-dependent protein interactions, many of which are prime drug targets, can lead to novel pharmacological intervention strategies. Therefore, the human kinase array approach is a versatile methodological addition, allowing to perform comprehensive studies of human kinases and their effects.

Materials and Methods

Antibodies

The following antibodies were used: mAB anti-phospho-CDK substrate (pTPXK, rabbit, Cell Signalling, 14371), mAB anti-phospho-CK2 substrate MultiMab™ ((pS/pT)DXE, rabbit, Cell Signalling, 8738), mAB anti-phospho- MAPK/CDK substrate (PXS*P or SPXR/K, rabbit, Cell Signalling, 2325), mAB anti-phospho-PKA substrate (RRXS*/T*, rabbit, Cell Signalling, 9624), pAB anti-phospho-(Ser)-PKC substrate ((R/K)X(S*)(Hyd)(R/K), rabbit, Cell Signalling, 2261), pAB anti-GST (goat, GEHealthcare, 27457701V), mAB anti-HA (mouse, Hiss Diagnostics GmbH, AB-10110), mAB anti-phospho-tyrosine clone 4G10 (mouse, Millipore, 05-321), secondary mAB anti-goat HRP (rabbit, Invitrogen, 611620), secondary mAB anti-mouse (sheep, GE Healthcare, LNA931V), secondary mAB anti-rabbit (donkey, GE Healthcare, LNA934V).

Yeast strains

BY4742 (MATα) MATα his3Δ1 leu2Δ0 lys2Δ0 ura3Δ0, (Winston *et al*, 1995; Brachmann *et al*, 1998); L40c (MATa) his3Δ200 trp1-901 leu2-3,112 LYS2::(lexAop)$_4$-HIS3 ura3::(lexAop)$_8$-lacZ ADE2::(lexAop)$_8$-URA3 GAL4 gal80 can1 cyh2 (Worseck *et al*, 2012); W303 (MATa/MATα) leu2-3,112 trp1-1 can1-100 ura3-1 ade2-1 his3-11,15 (Ralser *et al*, 2012); Y258 (MATa) pep4-3 his4-580 ura3-52 leu2-3 (Newman *et al*, 2013).

Growth phenotype screen

Dataset EV1 lists all conditions successfully tested including concentrations of additives. The four yeast strains were transformed with 1,020 clones (pASZ-C-DM or pASZ-CN-DM) representing kinases and protein set. For the growth phenotype screen, the kinase yeast array was transferred in 384 format using a gridding robot and grown on agar plates with minimal medium with 2% glucose and 20 µM CuSO$_4$ at 30°C unless otherwise stated (6–8 days). Yeast growth strength was visually evaluated in comparison to the overall growth of the yeast strain in the one condition and recorded using a 0–3 scale. According to this distribution, conditions which reduced growth of more than 175 colonies were excluded from further analysis (Dataset EV2)

Phospho-Y2H screen

The general Y2H set-up has been described in detail previously (Worseck *et al*, 2012). For the phospho-Y2H screen, the L40cα Y2H strain was cotransformed with the plasmids expressing the bait constructs (pBTM116-D9 or pBTMcC24-DM) and the prey constructs (pCBDU-JW or pACT4-DM). The independently transformed yeast colonies were mated with the L40c kinase array strains on YPD agar (30°C, 2 days). Active kinases modulating the phosphorylation-dependent PPI were identified by growth on selective media (SD5) supplemented with 20 µM or 100 µM CuSO$_4$ for the induction of kinase expression (30°C, 3–5 days).

Yeast growth curves

To measure yeast growth in liquid culture, triplicates of the W303 strain expressing a single human protein kinase were created on agar, transferred to liquid media in microtiter plate format. For the growth measurement, a 96-well MTP was incubated for 1 h at 30°C with orbital shaking, the yeast was then diluted with selective media (SD5, 500 µM CuSO$_4$) with or without 3.2% (v/v) DMSO to a starting OD$_{595}$ of 0.10-0.15. Then yeast growth was recorded in the MTP for 24 h by taking the OD every 10 min and shaking every hour for 5 min.

Protein interaction assays in mammalian cells

HEK293T cells were cultured in Dulbecco´s modified eagle medium (DMEM) with 10% fetal bovine serum (FBS) in a humidified 5% CO$_2$ atmosphere at 37°C. For the immunoprecipitation and pull-down experiments ~6 × 10^7 HEK293T cells were plated in a 10-cm cell culture dish and incubated for 24 prior to transfection. A total of 4 µg DNA of the different constructs were used for transfection with Lipofectamine 2000.

GST pull-down experiments form HEK293T cells (AAR2–PRPF8 interaction)

GST-tagged AAR2 (pcDNA5/FRT/TO-nGST) and the HA-Strep-tagged PRPF8 (pcDNA5/FRT/TO/SH/GW) constructs were cotransfected with PA-tagged kinase in HEK293T cells. HA-Strep-tagged PRPF8 protein was pulled down with Strep-Tactin Sepharose and the amount of bound AAR2 protein was determined by western

blotting. Cells were harvested 24 h after protein expression induction lysed in 0.5 ml LyseH-buffer (50 mM HEPES, 500 mM NaCl, 10% Glycerol, 0.5 mM EDTA, 2 mM MgCl$_2$, 1% NP-40, 12.1 mM sodium deoxycholate, 1× Phosphatase inhibitor III, 1× Protease inhibitor, 0.1 U/µl Benzonase), cleared, and incubated with human Strep-Tactin sepharose beads for 1 h on ice. The beads were washed four times with ice-cold WashH buffer (50 mM HEPES, 500 mM NaCl, 10% Glycerol, 0.5 mM EDTA, 2 mM MgCl$_2$, 1% NP-40, 12.1 mM sodium deoxycholate) and treated two times with 30 µl 2× SDS loading buffer for SDS–PAGE western blot analyses.

Immunoprecipitation of Erα

To analyze Erα phosphorylation in mammalian cells, PA-tagged Erα (pcDNA3.1PA-D57) was co-expressed with a GST-tagged kinase (pcDNA5/FRT/TO-nGST) in HEK293T cells, immunoprecipitated, and the phosphorylation status of ERα was analyzed with Pro-Q phospho-stain (Thermo Scientific) of SDS–PAGE. Transfected HEK293T cells were harvested 24 h after protein expression induction and lysed in 0.5 ml LyseH buffer for 30 min on ice. The cleared cell lysate was transferred onto prewashed 30 µl human IgG agarose beads and incubated 1 h on ice. The beads were washed four times with ice-cold WashH buffer and proteins were eluted with 30 µl 2× SDS loading buffer. After SDS gel electrophoresis, the gels were stained with Pro-Q Diamond phospho-stain and subsequent SYPRO Ruby whole protein stain and scanned with a fluorescence scanner according to the manufacturer's instructions.

GST pull-down experiments form HEK293T cells (Erα–14-3-3 interaction)

GST-tagged 14-3-3 constructs (pDESTcoG) were expressed in *E. coli*, then loaded on GST-coated beads and incubated with HEK293T cell lysate containing co-expressed PA-tagged ERα and GST-tagged kinases. The amount coprecipitated ERα was detected by western blotting. GST-tagged 14-3-3 was expressed in 12 ml *E. coli* culture (TB-medium, 100 µg/ml ampicillin, 30 µg/ml chloramphenicol) for about 20 h at 37°C and 150 rpm shaking. *E. coli* cells were lysed in 1.85 ml LyseB buffer (50 mM HEPES, 5400 mM NaCl, 5% Glycerol, 1 mM EDTA, 0.5% Brij58, 1 mg/ml Lysozyme, 2 mM DTT). 0.1 U/µl Benzonase was added in 50 mM HEPES pH 8, 2 mM MgCl$_2$ and incubated for 30 min at 4°C. 9 µl supernatant with expressed 14-3-3β was used for the pull-down experiment with 5 µl human Glutathione magnetic beads pre-incubated with 100 µl LyseH buffer each. The HEK293T cell lysates were prepared 24 h after protein expression induction in 0.5 ml LyseH-buffer mixed with the GST-fusion beads with the bound 14-3-3 proteins and incubated on ice for 1 h. The beads were washed six times with 0.5 ml ice-cold WashH buffer and samples were eluted from the beads with 30 µl 2× SDS loading buffer. Samples were subject to SDS gel electrophoresis and subsequent western blotting.

Co-immunoprecipitation with luciferase readout

Luciferase-based co-immunoprecipitation experiments were performed in HEK293T cells in 96-well format using 150 ng of plasmid DNA in total (firefly-V5 fusion 14-3-3β construct in pcDNA3.1V5Fire-DM and kinase protein A fusion constructs in pcDNA3.1PA-D57) as described previously (Hegele *et al*, 2012; Woodsmith *et al*, 2018).

Transient transfection for luciferase transcription assays and FACS

The cells were seeded out in phenol red—free DMEM supplemented with 10% charcoal stripped FBS on 96-well plates. For each condition, 24 h after seeding the cells were transfected with 500 ng total expression plasmid (kinase/kinase-dead (GST-tagged) as indicated, filled up to 500 ng with a corresponding empty vector), 25 ng ERα (PA-tagged) expression plasmid, and 500 ng pGL3-(ERE)$_2$-LUC per 6 wells (technical replicates), using PEI method. For MCF7 cells, ERα was omitted. PEI to DNA ratio was 5:1 w/w or 2.5:1 for HEK293T and MCF7 or U2-OS, respectively. Six hours after transfection, the medium was changed, and the cells were stimulated with 1 nM E2 (17β-estradiol). 24 h after transfection, the cells were washed and lysed in Luciferase Cell Culture Lysis Reagent (Promega). The luciferase activity was quantitated using Luciferase Assay System (Promega) and a microplate reader (DTX800) and normalized to the protein content. For the control FACS experiments, HEK293T were transfected as described above, but in a 12-well format, with indicated DNA amounts per well of a 12-well plate. 24 h post-transfection, the cells were trypsinized, transferred to FACS tubes at 10^6 cells/100 µl, and the cellular DNA was stained with 20 µg/ml Hoechst 33258 for 1 h at 37°C in the dark. The staining was stopped by transferring the cell suspension on ice. The DNA content of the cells was measured using 355 nm UV laser and 450/45 nm DAPI filter.

Data processing and visualization

Data processing, statistical analyses, and visualization was performed in R. Cell cycle analysis based on the DNA content was performed using commercially available ModFit LT software. Kinome tree graphics were produced using CORAL at http://phanstiel-lab.med.unc.edu/CORAL/.

Data availability

The datasets generated in this study are available as Datasets EV1–EV4.

Expanded View for this article is available online.

Author contributions

Stefanie Jehle: Formal analysis; Validation; Investigation; Visualization; Methodology; Writing—review and editing. **Natalia Kunowska:** Formal analysis; Validation; Investigation; Visualization; Writing—review and editing. **Nouhad Benlasfer:** Validation; Investigation. **Jonathan Woodsmith:** Formal analysis; Visualization; Methodology; Writing—review and editing. **Gert Weber:** Investigation; Visualization; Writing—review and editing. **Markus C Wahl:** Resources; Supervision; Funding acquisition; Writing—review and editing. **Ulrich Stelzl:** Conceptualization; Resources;

Formal analysis; Supervision; Funding acquisition; Visualization; Methodology; Writing—original draft; Writing—review and editing.

Disclosure and competing interests statement

The authors declare that they have no conflict of interest.

References

Absmeier E, Rosenberger L, Apelt L, Becke C, Santos KF, Stelzl U, Wahl MC (2015) A noncanonical PWI domain in the N-terminal helicase-associated region of the spliceosomal Brr2 protein. *Acta Crystallogr* 71: 762–771

Ahler E, Register AC, Chakraborty S, Fang L, Dieter EM, Sitko KA, Vidadala RSR, Trevillian BM, Golkowski M, Gelman H *et al* (2019) A combined approach reveals a regulatory mechanism coupling Src's kinase activity, localization, and phosphotransferase-independent functions. *Mol Cell* 74: 393–408.e20

Alessi DR, Andjelkovic M, Caudwell B, Cron P, Morrice N, Cohen P, Hemmings BA (1996) Mechanism of activation of protein kinase B by insulin and IGF-1. *EMBO J* 15: 6541–6551

Anastassiadis T, Deacon SW, Devarajan K, Ma H, Peterson JR (2011) Comprehensive assay of kinase catalytic activity reveals features of kinase inhibitor selectivity. *Nat Biotechnol* 29: 1039–1045

Anbalagan M, Rowan BG (2015) Estrogen receptor alpha phosphorylation and its functional impact in human breast cancer. *Mol Cell Endocrinol* 418(Pt 3): 264–272

Berginski ME, Moret N, Liu C, Goldfarb D, Sorger PK, Gomez SM (2021) The Dark Kinase Knowledgebase: an online compendium of knowledge and experimental results of understudied kinases. *Nucleic Acids Res* 49: D529–D535

Boschelli F, Uptain SM, Lightbody JJ (1993) The lethality of p60v-src in *Saccharomyces cerevisiae* and the activation of p34CDC28 kinase are dependent on the integrity of the SH2 domain. *J Cell Sci* 105(Pt 2): 519–528

Brachmann CB, Davies A, Cost GJ, Caputo E, Li J, Hieter P, Boeke JD (1998) Designer deletion strains derived from Saccharomyces cerevisiae S288C: a useful set of strains and plasmids for PCR-mediated gene disruption and other applications. *Yeast* 14: 115–132

Brugge JS, Jarosik G, Andersen J, Queral-Lustig A, Fedor-Chaiken M, Broach JR (1987) Expression of Rous sarcoma virus transforming protein pp60v-src in *Saccharomyces cerevisiae* cells. *Mol Cell Biol* 7: 2180–2187

Campbell J, Ryan C, Brough R, Bajrami I, Pemberton H, Chong I, Costa-Cabral S, Frankum J, Gulati A, Holme H *et al* (2016) Large-scale profiling of kinase dependencies in cancer cell lines. *Cell Rep* 14: 2490–2501

Cau J, Faure S, Comps M, Delsert C, Morin N (2001) A novel p21-activated kinase binds the actin and microtubule networks and induces microtubule stabilization. *J Cell Biol* 155: 1029–1042

Cohen P, Cross D, Jänne PA (2021) Kinase drug discovery 20 years after imatinib: progress and future directions. *Nat Rev Drug Discovery* 20: 551–569

Cooper JA, MacAuley A (1988) Potential positive and negative autoregulation of p60c-src by intermolecular autophosphorylation. *Proc Natl Acad Sci USA* 85: 4232–4236

Corwin T, Woodsmith J, Apelt F, Fontaine J-F, Meierhofer D, Helmuth J, Grossmann A, Andrade-Navarro MA, Ballif BA, Stelzl U (2017) Defining human tyrosine kinase phosphorylation networks using yeast as an *in vivo* model substrate. *Cell Syst* 5: 128–139

De Vries-van Leeuwen IJ, da Costa Pereira D, Flach KD, Piersma SR, Haase C, Bier D, Yalcin Z, Michalides R, Feenstra KA, Jimenez CR *et al* (2013) Interaction of 14-3-3 proteins with the estrogen receptor alpha F domain provides a drug target interface. *Proc Natl Acad Sci USA* 110: 8894–8899

Dörr J, Kartarius S, Götz C, Montenarh M (2008) Contribution of the individual subunits of protein kinase CK2 and of hPrp3p to the splicing process. *Mol Cell Biochem* 316: 187–193

Dowell RD, Ryan O, Jansen A, Cheung D, Agarwala S, Danford T, Bernstein DA, Rolfe PA, Heisler LE, Chin B *et al* (2010) Genotype to phenotype: a complex problem. *Science* 328: 469

Elkins JM, Fedele V, Szklarz M, Abdul Azeez KR, Salah E, Mikolajczyk J, Romanov S, Sepetov N, Huang X-P, Roth BL *et al* (2016) Comprehensive characterization of the published kinase inhibitor set. *Nat Biotechnol* 34: 95–103

Elledge SJ, Spottswood MR (1991) A new human p34 protein kinase, CDK2, identified by complementation of a cdc28 mutation in *Saccharomyces cerevisiae*, is a homolog of Xenopus Eg1. *EMBO J* 10: 2653–2659

Enzler F, Tschaikner P, Schneider R, Stefan E (2020) KinCon: cell-based recording of full-length kinase conformations. *IUBMB Life* 72: 1168–1174

Fedorov O, Müller S, Knapp S (2010) The (un)targeted cancer kinome. *Nat Chem Biol* 6: 166–169

Filhol O, Cochet C (2009) Protein kinase CK2 in health and disease: cellular functions of protein kinase CK2: a dynamic affair. *Cell Mol Life Sci* 66: 1830–1839

Filteau M, Vignaud H, Rochette S, Diss G, Chrétien A-È, Berger CM, Landry CR (2016) Multi-scale perturbations of protein interactomes reveal their mechanisms of regulation, robustness and insights into genotype-phenotype maps. *Brief Funct Genomics* 15: 130–137

Florio M, Wilson LK, Trager JB, Thorner J, Martin GS (1994) Aberrant protein phosphorylation at tyrosine is responsible for the growth-inhibitory action of pp60v-src expressed in the yeast *Saccharomyces cerevisiae*. *Mol Biol Cell* 5: 283–296

Galej WP, Oubridge C, Newman AJ, Nagai K (2013) Crystal structure of Prp8 reveals active site cavity of the spliceosome. *Nature* 493: 638–643

Grossmann A, Benlasfer N, Birth P, Hegele A, Wachsmuth F, Apelt L, Stelzl U (2015) Phospho-tyrosine dependent protein-protein interaction network. *Mol Syst Biol* 11: 794

Hall JM, McDonnell DP (1999) The estrogen receptor beta-isoform (ERbeta) of the human estrogen receptor modulates ERalpha transcriptional activity and is a key regulator of the cellular response to estrogens and antiestrogens. *Endocrinology* 140: 5566–5578

Harris LK, Frumm SM, Bishop AC (2013) A general assay for monitoring the activities of protein tyrosine phosphatases in living eukaryotic cells. *Anal Biochem* 435: 99–105

Hegele A, Kamburov A, Grossmann A, Sourlis C, Wowro S, Weimann M, Will CL, Pena V, Lührmann R, Stelzl U (2012) Dynamic protein-protein interaction wiring of the human spliceosome. *Mol Cell* 45: 567–580

Hillenmeyer ME, Fung E, Wildenhain J, Pierce SE, Hoon S, Lee W, Proctor M, St Onge RP, Tyers M, Koller D *et al* (2008) The chemical genomic portrait of yeast: uncovering a phenotype for all genes. *Science* 320: 362–365

Hornbeck PV, Kornhauser JM, Tkachev S, Zhang B, Skrzypek E, Murray B, Latham V, Sullivan M (2012) PhosphoSitePlus: a comprehensive resource for investigating the structure and function of experimentally determined post-translational modifications in man and mouse. *Nucleic Acids Res* 40: D261–D270

Huang S, Zhu Y, Wang C, Li X, Cui X, Tu S, You L, Fu J, Chen Z, Hu W *et al* (2020) PAK5 facilitates the proliferation, invasion and migration in colorectal cancer cells. *Cancer Med* 9: 4777–4790

Kanev GK, de Graaf C, de Esch IJP, Leurs R, Würdinger T, Westerman BA, Kooistra AJ (2019) The landscape of atypical and eukaryotic protein kinases. *Trends Pharmacol Sci* 40: 818–832

Kang J, Yang M, Li B, Qi W, Zhang C, Shokat KM, Tomchick DR, Machius M, Yu H (2008) Structure and substrate recruitment of the human spindle checkpoint kinase Bub1. *Mol Cell* 32: 394–405

Kim J-H, Seo Y, Jo M, Jeon H, Lee W-H, Yachie N, Zhong Q, Vidal M, Roth FP, Suk K (2020) Yeast-based genetic interaction analysis of human kinome. *Cells* 9: 1156

Kobayashi T, Cohen P (1999) Activation of serum- and glucocorticoid-regulated protein kinase by agonists that activate phosphatidylinositide 3-kinase is mediated by 3-phosphoinositide-dependent protein kinase-1 (PDK1) and PDK2. *Biochem J* 339(Pt 2): 319–328

van de Kooij B, Creixell P, van Vlimmeren A, Joughin BA, Miller CJ, Haider N, Simpson CD, Linding R, Stambolic V, Turk BE *et al* (2019) Comprehensive substrate specificity profiling of the human Nek kinome reveals unexpected signaling outputs. *eLife* 8: e44635

Kornbluth S, Jove R, Hanafusa H (1987) Characterization of avian and viral p60src proteins expressed in yeast. *Proc Natl Acad Sci USA* 84: 4455–4459

Koyama M, Saito S, Nakagawa R, Katsuyama I, Hatanaka M, Yamamoto T, Arakawa T, Tokunag M (2006) Expression of human tyrosine kinase, Lck, in yeast *Saccharomyces cerevisiae*: growth suppression and strategy for inhibitor screening. *Protein Pept Lett* 13: 915–920

Kritzer JA, Freyzon Y, Lindquist S (2018) Yeast can accommodate phosphotyrosine: V-Src toxicity in yeast arises from a single disrupted pathway. *FEMS Yeast Res* 18: foy027

Lehnert S, Götz C, Kartarius S, Schäfer B, Montenarh M (2008) Protein kinase CK2 interacts with the splicing factor hPrp3p. *Oncogene* 27: 2390–2400

Malumbres M, Harlow E, Hunt T, Hunter T, Lahti JM, Manning G, Morgan DO, Tsai L-H, Wolgemuth DJ (2009) Cyclin-dependent kinases: a family portrait. *Nat Cell Biol* 11: 1275–1276

Manning G, Whyte DB, Martinez R, Hunter T, Sudarsanam S (2002) The protein kinase complement of the human genome. *Science* 298: 1912–1934

Meggio F, Pinna LA (2003) One-thousand-and-one substrates of protein kinase CK2? *FASEB J* 17: 349–368

Moesslacher CS, Kohlmayr JM, Stelzl U (2021) Exploring absent protein function in yeast: assaying post translational modification and human genetic variation. *Microbial Cell* 8: 164–183

Nada S, Okada M, MacAuley A, Cooper JA, Nakagawa H (1991) Cloning of a complementary DNA for a protein-tyrosine kinase that specifically phosphorylates a negative regulatory site of p60c-src. *Nature* 351: 69–72

Needham EJ, Parker BL, Burykin T, James DE, Humphrey SJ (2019) Illuminating the dark phosphoproteome. *Sci Signal* 12: eaau8645

Newman RH, Hu J, Rho H-S, Xie Z, Woodard C, Neiswinger J, Cooper C, Shirley M, Clark HM, Hu S *et al* (2013) Construction of human activity-based phosphorylation networks. *Mol Syst Biol* 9: 655

Ninomiya-Tsuji J, Nomoto S, Yasuda H, Reed SI, Matsumoto K (1991) Cloning of a human cDNA encoding a CDC2-related kinase by complementation of a budding yeast cdc28 mutation. *Proc Natl Acad Sci USA* 88: 9006–9010

Nishi H, Hashimoto K, Panchenko AR (2011) Phosphorylation in protein-protein binding: effect on stability and function. *Structure* 19: 1807–1815

Nuñez de Villavicencio-Diaz T, Rabalski AJ, Litchfield DW (2017) Protein kinase CK2: intricate relationships within regulatory cellular networks. *Pharmaceuticals* 10: 27

O'Regan L, Fry AM (2009) The Nek6 and Nek7 protein kinases are required for robust mitotic spindle formation and cytokinesis. *Mol Cell Biol* 29: 3975–3990

Ochoa D, Jonikas M, Lawrence RT, El Debs B, Selkrig J, Typas A, Villén J, Santos SD, Beltrao P (2016) An atlas of human kinase regulation. *Mol Syst Biol* 12: 888

Pao AC (2012) SGK regulation of renal sodium transport. *Curr Opin Nephrol Hypertens* 21: 534–540

Piñero J, Saüch J, Sanz F, Furlong LI (2021) The DisGeNET cytoscape app: exploring and visualizing disease genomics data. *Comput Struct Biotechnol J* 19: 2960–2967

Ralser M, Kuhl H, Ralser M, Werber M, Lehrach H, Breitenbach M, Timmermann B (2012) The *Saccharomyces cerevisiae* W303–K6001 cross-platform genome sequence: Insights into ancestry and physiology of a laboratory mutt. *Open Biol* 2: 120093

Ranzuglia V, Lorenzon I, Pellarin I, Sonego M, Dall'Acqua A, D'Andrea S, Lovisa S, Segatto I, Coan M, Polesel J *et al* (2020) Serum- and glucocorticoid- inducible kinase 2, SGK2, is a novel autophagy regulator and modulates platinum drugs response in cancer cells. *Oncogene* 39: 6370–6386

Rodríguez-Escudero I, Andrés-Pons A, Pulido R, Molina M, Cid VJ (2009) Phosphatidylinositol 3-kinase-dependent activation of mammalian protein kinase B/Akt in Saccharomyces cerevisiae, an in vivo model for the functional study of Akt mutations. *J Biol Chem* 284: 13373–13383

Santos K, Preussner M, Heroven AC, Weber G (2015) Crystallization and biochemical characterization of the human spliceosomal Aar2-Prp8 (RNaseH) complex. *Acta Crystallogr* 71: 1421–1428

Schmitt DL, Mehta S, Zhang J (2020) Illuminating the kinome: visualizing real-time kinase activity in biological systems using genetically encoded fluorescent protein-based biosensors. *Curr Opin Chem Biol* 54: 63–69

Sekigawa M, Kunoh T, Wada S-I, Mukai Y, Ohshima K, Ohta S, Goshima N, Sasaki R, Mizukami T (2010) Comprehensive screening of human genes with inhibitory effects on yeast growth and validation of a yeast cell-based system for screening chemicals. *J Biomol Screen* 15: 368–378

Shults MD, Janes KA, Lauffenburger DA, Imperiali B (2005) A multiplexed homogeneous fluorescence-based assay for protein kinase activity in cell lysates. *Nat Methods* 2: 277–283

Taipale M, Krykbaeva I, Whitesell L, Santagata S, Zhang J, Liu Q, Gray NS, Lindquist S (2013) Chaperones as thermodynamic sensors of drug-target interactions reveal kinase inhibitor specificities in living cells. *Nat Biotechnol* 31: 630–637

Tan CSH, Bodenmiller B, Pasculescu A, Jovanovic M, Hengartner MO, Jørgensen C, Bader GD, Aebersold R, Pawson T, Linding R (2009a) Comparative analysis reveals conserved protein phosphorylation networks implicated in multiple diseases. *Sci Signal* 2: ra39

Tan CSH, Pasculescu A, Lim WA, Pawson T, Bader GD, Linding R (2009b) Positive selection of tyrosine loss in metazoan evolution. *Science* 325: 1686–1688

Tinti M, Madeira F, Murugesan G, Hoxhaj G, Toth R, Mackintosh C (2014) ANIA: ANnotation and Integrated Analysis of the 14-3-3 interactome. *Database* 2014: bat085

Trembley JH, Tatsumi S, Sakashita E, Loyer P, Slaughter CA, Suzuki H, Endo H, Kidd VJ, Mayeda A (2005) Activation of pre-mRNA splicing by human RNPS1 is regulated by CK2 phosphorylation. *Mol Cell Biol* 25: 1446–1457

Tudor CO, Ross KE, Li G, Vijay-Shanker K, Wu CH, Arighi CN (2015) Construction of phosphorylation interaction networks by text mining of full-length articles using the eFIP system. *Database* 2015: bav020

Ubersax JA, Ferrell JE (2007) Mechanisms of specificity in protein phosphorylation. *Nat Rev Mol Cell Biol* 8: 530–541

Vinayagam A, Stelzl U, Wanker EE (2010) Repeated two-hybrid screening detects transient protein–protein interactions. *Theor Chem Acc* 125: 613–619

Wahl MC, Will CL, Lührmann R (2009) The spliceosome: design principles of a dynamic RNP machine. *Cell* 136: 701–718

Wang M, Herrmann CJ, Simonovic M, Szklarczyk D, von Mering C (2015) Version 4.0 of PaxDb: Protein abundance data, integrated across model organisms, tissues, and cell-lines. *Proteomics* 15: 3163−3168

Weber G, Cristão VF, de L. Alves F, Santos KF, Holton N, Rappsilber J, Beggs JD, Wahl MC (2011) Mechanism for Aar2p function as a U5 snRNP assembly factor. *Genes Dev* 25: 1601−1612

Weber G, Cristão VF, Santos KF, Jovin SM, Heroven AC, Holton N, Lührmann R, Beggs JD, Wahl MC (2013) Structural basis for dual roles of Aar2p in U5 snRNP assembly. *Genes Dev* 27: 525−540

Weimann M, Grossmann A, Woodsmith J, Özkan Z, Birth P, Meierhofer D, Benlasfer N, Valovka T, Timmermann B, Wanker EE *et al* (2013) A Y2H-seq approach defines the human protein methyltransferase interactome. *Nat Methods* 10: 339−342

Winston F, Dollard C, Ricupero-Hovasse SL (1995) Construction of a set of convenient *Saccharomyces cerevisiae* strains that are isogenic to S288C. *Yeast* 11: 53−55

Woodsmith J, Stelzl U (2014) Studying post-translational modifications with protein interaction networks. *Curr Opin Struct Biol* 24: 34−44

Woodsmith J, Apelt L, Casado-Medrano V, Özkan Z, Timmermann B, Stelzl U (2017) Protein interaction perturbation profiling at amino-acid resolution. *Nat Methods* 14: 1213−1221

Woodsmith J, Casado-Medrano V, Benlasfer N, Eccles RL, Hutten S, Heine CL, Thormann V, Abou-Ajram C, Rocks O, Dormann D *et al* (2018) Interaction modulation through arrays of clustered methyl-arginine protein modifications. *Life Sci Alliance* 1: e201800178

Worseck JM, Grossmann A, Weimann M, Hegele A, Stelzl U (2012) A stringent yeast two-hybrid matrix screening approach for protein-protein interaction discovery. *Methods Mol Biol* 812: 63−87

Yang F, Sun S, Tan G, Costanzo M, Hill DE, Vidal M, Andrews BJ, Boone C, Roth FP (2017) Identifying pathogenicity of human variants via paralog-based yeast complementation. *PLoS Genet* 13: e1006779

Yin M-J, Shao L, Voehringer D, Smeal T, Jallal B (2003) The serine/threonine kinase Nek6 is required for cell cycle progression through mitosis. *J Biol Chem* 278: 52454−52460

Zhang J, Allen MD (2007) FRET-based biosensors for protein kinases: illuminating the kinome. *Mol BioSyst* 3: 759−765